CHALMERS
FINITE ELEMENT CENTER

PREPRINT 2001-01

A Simple Nonconforming Bilinear Element for the Elasticity Problem

Peter Hansbo and Mats G. Larson

Chalmers Finite Element Center
CHALMERS UNIVERSITY OF TECHNOLOGY
Göteborg Sweden 2001

CHALMERS FINITE ELEMENT CENTER

Preprint 2001-01

A Simple Nonconforming Bilinear Element for the Elasticity Problem

Peter Hansbo and Mats G. Larson

CHALMERS

Chalmers Finite Element Center
Chalmers University of Technology
SE–412 96 Göteborg Sweden
Göteborg, January 2001

A Simple Nonconforming Bilinear Element for the Elasticity Problem
Peter Hansbo and Mats G. Larson
NO 2001-01
ISSN 1404–4382

Chalmers Finite Element Center
Chalmers University of Technology
SE–412 96 Göteborg
Sweden
Telephone: +46 (0)31 772 1000
Fax: +46 (0)31 772 3595
`www.phi.chalmers.se`

Printed in Sweden
Chalmers University of Technology
Göteborg, Sweden 2001

A Simple Nonconforming Bilinear Element for the Elasticity Problem *

Peter Hansbo† and Mats G. Larson‡

January 29, 2001

Abstract

We look at the mixed non-conforming Rannacher-Turek (RT) element from the point of view of discontinuous Galerkin methods. In the case of the elasticity operator, for which the RT element is not stable in that it does not (in general) fulfill a discrete Korn's inequality, the discontinuous framework naturally suggests the appearance of (weakly consistent) stabilization terms. We thus obtain a modifed, stable and locking free, version of the RT element for the elasticity problem. We also give some implementation aspects of the element. Numerical results are included.

1 Introduction

Bi– or trilinear elements are often preferred to simplex elements since the former yield more approximating power per degree of freedom. In the case of (nearly) incompressible materials, the Q1P0–element, using a bi/tri-linear approximation of the displacements and a constant approximation of the "pressure", is often used. Unfortunately, this element is not quite stable, although it usually performs quite well. An alternative is the Rannacher-Turek (RT) element, a simple non-conforming finite element method for bi– or trilinear elements with nodes situated at the midpoints of the element sides. It was introduced for Stokes problem by Rannacher and Turek [7] in combination with piecewise constant pressures. However, for the traction problem in elasticity it is not fully stable. A simple way of seeing this is to use the argument given by Hughes [5] for the Crouzeix-Raviart element: prescribing the displacements along one side of an element means prescribing the displacement in only one node, which cannot preclude rigid body rotations.

*To appear in *Trends in Computational Structural Mechanics*, W.A. Wall, K.-U. Bletzinger, and K. Schweizerkopf (Eds.), CIMNE, Barcelona, Spain 2001

†Department of Solid Mechanics Chalmers University of Technology S–412 96 Göteborg, Sweden, email:hansbo@solid.chalmers.se

‡Department of Mathematics Chalmers University of Technology S–412 96 Göteborg, Sweden, email:mgl@math.chalmers.se

In this paper, we suggest a simple modification of the RT element, motivated by Nitsche's method [6], which introduces stability without sacrificing accuracy. This means that the modified RT element can be used for the elasticity operator (which is the physically correct operator also in the case of fluid dynamics), and that it will not lock in the incompressible limit.

2 The equations of elasticity

We consider the equations of linear elasticity in two dimensions: Find the displacement $\boldsymbol{u} = [u_i]_{i=1}^2$ and the symmetric stress tensor $\boldsymbol{\sigma} = [\sigma_{ij}]_{i,j=1}^2$ such that

$$\begin{aligned} \boldsymbol{\sigma} = \lambda\ \nabla \cdot \boldsymbol{u} \boldsymbol{I} + 2\mu\boldsymbol{\varepsilon}(\boldsymbol{u}) \quad & \text{in } \Omega, \\ -\nabla \cdot \boldsymbol{\sigma} = \boldsymbol{f} \quad & \text{in } \Omega, \\ \boldsymbol{u} = \boldsymbol{0} \quad & \text{on } \partial\Omega_{\mathrm{D}}, \\ \boldsymbol{\sigma} \cdot \boldsymbol{n} = \boldsymbol{h} \quad & \text{on } \partial\Omega_{\mathrm{N}}. \end{aligned} \tag{1}$$

Here λ and μ are positive constants called the Lamé constants, satisfying $0 < \mu_1 < \mu < \mu_2$ and $0 < \lambda < \infty$, and $\boldsymbol{\varepsilon}(\boldsymbol{u}) = [\varepsilon_{ij}(\boldsymbol{u})]_{i,j=1}^2$ is the strain tensor with components

$$\varepsilon_{ij}(\boldsymbol{u}) = \frac{1}{2}\left(\frac{\partial u_i}{\partial x_j} + \frac{\partial u_j}{\partial x_i}\right).$$

Furthermore, $\nabla \cdot \boldsymbol{\sigma} = \left[\sum_{j=1}^2 \partial\sigma_{ij}/\partial x_j\right]_{i=1}^2$, $\boldsymbol{I} = [\delta_{ij}]_{i,j=1}^2$ with $\delta_{ij} = 1$ if $i = j$ and $\delta_{ij} = 0$ if $i \neq j$, $\boldsymbol{f}$ and $\boldsymbol{h}$ are given loads, $\boldsymbol{g}$ is a given boundary displacement, and $\boldsymbol{n}$ is the outward unit normal to $\partial\Omega$. In terms of the modulus of elasticity, E, and Poisson's ratio, ν, we have, in the case of plane strain, that $\lambda = E\nu/((1+\nu)(1-2\nu))$ and $\mu = E/(2(1+\nu))$.

We shall consider a mixed approximation for the solution of (1), so we introduce an auxiliary scalar field p and formulate the elasticity problem as follows: Find the displacement $\boldsymbol{u} = [u_i]_{i=1}^2$ and the "pressure" p such that

$$\begin{aligned} -\nabla \cdot (2\mu\boldsymbol{\varepsilon}(\boldsymbol{u}) - p\,\boldsymbol{I}) = \boldsymbol{f} \quad & \text{in } \Omega, \\ \frac{1}{\lambda}p + \nabla \cdot \boldsymbol{u} = 0 \quad & \text{in } \Omega, \\ \boldsymbol{u} = \boldsymbol{0} \quad & \text{on } \partial\Omega_{\mathrm{D}}, \\ (2\mu\boldsymbol{\varepsilon}(\boldsymbol{u}) - p\,\boldsymbol{I}) \cdot \boldsymbol{n} = \boldsymbol{h} \quad & \text{on } \partial\Omega_{\mathrm{N}}. \end{aligned} \tag{2}$$

Incompressible behavior is obtained as the parameter $\lambda \to \infty$, i.e., as $\nu \to 1/2$. In such cases standard (low order) methods will lock. In [7], the RT element was shown not to lock in the case of Stokes' problem, where $\lambda \to \infty$ and $-\nabla \cdot (2\mu\boldsymbol{\varepsilon}(\boldsymbol{u}))$ is replaced by $-\mu\Delta\boldsymbol{u}$. However, for (2), which is the correct form of the equations of elasticity in the general case, the RT element cannot control the rigid body rotations, which leads to instability, cf. Hughes [5]. Here, we will instead view the RT element as a special choice of discretization in a discontinuous Galerkin framework following the approach suggested by Hansbo and Larson [3] for the Crouzeix-Raviart element, which will lead to a stable element for (2).

3 The Rannacher-Turek approximation in a discontinuous Galerkin framework

3.1 A parametric version of the nonparametric Rannacher-Turek element

We shall focus on the two-dimensional case, but the formulation of the method in three dimensions follows the same pattern. Thus, consider a subdivision of a bounded region $\Omega \subset \mathbb{R}^2$ into a geometrically conforming finite element partitioning $\mathcal{T}_h = \{T\}$ of Ω consisting of convex quadrilaterals. In [7], Rannacher and Turek give the following nonparametric definition of a nonconforming bilinear element: for any element $T \in \mathcal{T}_h$, let $(\bar{\xi}, \bar{\eta})$ denote a coordinate system obtained by joining the midpoints of the opposing faces of T. On each T we set

$$Q_1(T) := \mathrm{span}\{1, \bar{\xi}, \bar{\eta}, \bar{\xi}^2 - \bar{\eta}^2\}.$$

One can now choose what type of continuity one wants. Denoting by Γ^i the faces of the element and $\boldsymbol{m}^i$ the midpoints of the faces, natural choices are

a) continuity in the mean, symbolized by the nodal functional $F^a_{\Gamma^i}(\boldsymbol{v}) = |\Gamma^i|^{-1} \int_{\Gamma^i} \boldsymbol{v}\, ds$.

b) continuity at the midpoints of the faces, symbolized by the nodal functional $F^b_{\Gamma^i}(\boldsymbol{v}) = \boldsymbol{v}(\boldsymbol{m}^i)$.

The corresponding approximating spaces that will be used for the displacements are

$$\begin{aligned}\boldsymbol{W}^h_{a/b} \;:=\; & \{\boldsymbol{v} \in [L_2(\Omega)]^2 : \boldsymbol{v} \in Q_1(T), \forall T \in \mathcal{T}_h, \boldsymbol{v} \text{ is continuous w.r.t.} \\ & \text{all the functionals } F^{a/b}_{\Gamma^i}, \text{ and } F^{a/b}_{\Gamma^i} = 0 \text{ if } \Gamma^i \subset \partial\Omega_D\}.\end{aligned}$$

For the pressure, we will use the space

$$L^h := \{q_h \in L_2(\Omega)) : \; q_h|_T \in P_0, \forall T \in \mathcal{T}_h\},$$

where P_0 is the space of constants. In [7], it is shown that $\boldsymbol{W}^h_a$ is less sensitive to mesh distortion than $\boldsymbol{W}^h_b$ when solving the Stokes problem, but that both are stable with respect to the Babuška-Brezzi condition.

There is a parametric version of $Q_1(T)$, which means that there exists a reference configuration for the approximation (a fact not noted in [7]). There is also the possibility of expressing the approximation in global coordinates (x, y), which simplifies the implementation. To define the reference configuration, we must separate the geometry (based on the usual bilinear map) from the approximation itself. Consider thus a reference element defined for $0 \le \xi \le 1$, $0 \le \eta \le 1$. Using the double node/side numbering of Figure 1, we use superscripts to denote quantities associated with sides, so that $\{\boldsymbol{m}^i\}$ denotes the physical location of the side midpoints, and $\{\phi^i\}$ denotes the nonconforming basis functions, and subscripts to denote quantities related to the corners, so that $\{\boldsymbol{x}_i\}$ denotes the physical location of the corners. The local basis for the approximation space $\boldsymbol{W}_b^h$ is given by

$$\begin{aligned}\phi^1 &= 3/4 + \xi - \xi^2 - 2\eta + \eta^2,\\ \phi^2 &= -1/4 + \xi^2 + \eta - \eta^2,\\ \phi^3 &= -1/4 + \xi - \xi^2 + \eta^2,\\ \phi^4 &= 3/4 - 2\xi + \xi^2 + \eta - \eta^2.\end{aligned}$$

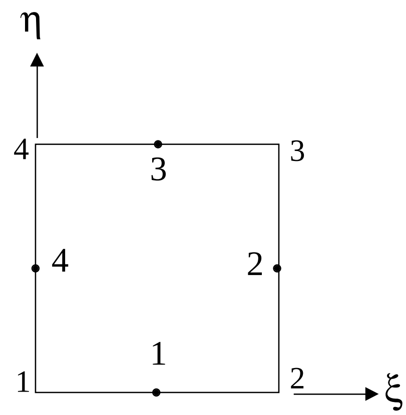

Figure 1: Reference element $\hat{T}$.

The map $\boldsymbol{F} : (\xi, \eta) \to (x, y)$ to be used in the following can then be defined as

$$(x, y) = \boldsymbol{F}(\xi, \eta) := \sum_i \phi^i(\xi, \eta)\boldsymbol{m}^i.$$

We next state the crucial property of the map $\boldsymbol{F}$, illustrated in Figure 2.

Lemma 3.1 *The map* $\boldsymbol{F}$ *is affine.*

Proof. We have that $\boldsymbol{m}^1 = (\boldsymbol{x}_1 + \boldsymbol{x}_2)/2$, $\boldsymbol{m}^2 = (\boldsymbol{x}_2 + \boldsymbol{x}_3)/2$, $\boldsymbol{m}^3 = (\boldsymbol{x}_3 + \boldsymbol{x}_4)/2$ and $\boldsymbol{m}^3 = (\boldsymbol{x}_4 + \boldsymbol{x}_1)/2$, so a straightforward computation shows that

$$\boldsymbol{x}(\boldsymbol{\xi}) = \frac{(\boldsymbol{x}_2 + \boldsymbol{x}_3 - \boldsymbol{x}_1 - \boldsymbol{x}_4)\xi}{2} + \frac{(\boldsymbol{x}_3 + \boldsymbol{x}_4 - \boldsymbol{x}_1 - \boldsymbol{x}_2)\eta}{2} + \frac{3\boldsymbol{x}_1 + \boldsymbol{x}_2 - \boldsymbol{x}_3 + \boldsymbol{x}_4}{4}.$$

i.e., the map is affine. □

Corollary 3.2 *The map between* $(\bar{\xi}, \bar{\eta})$*, used in [7], and* (ξ, η) *is affine and given by*

$$\bar{\xi} = \frac{x_1 + x_4}{2} + \left(\frac{x_2 + x_3}{2} - \frac{x_1 + x_4}{2}\right)\xi \quad \textit{and} \quad \bar{\eta} = \frac{y_1 + y_2}{2} + \left(\frac{y_3 + y_4}{2} - \frac{y_1 + y_2}{2}\right)\eta.$$

Thus the approximating properties of the resulting elements are identical.

Remark 3.3 *The geometrical object obtained when using* $\boldsymbol{F}$ *to map* $(0,1)\times(0,1)$ *is called the* equivalent parallelogram *by Arunakirinathar and Reddy [2], who use a different, but equivalent, definition of* $\boldsymbol{F}$*.*

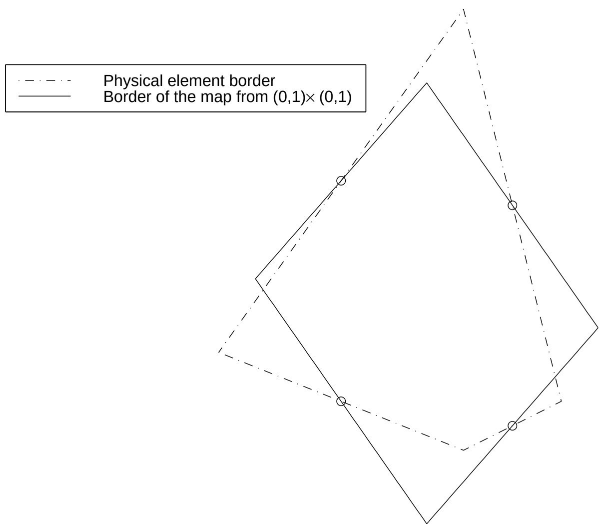

Figure 2: Mapped element.

4 Construction of the element

Since the map $\boldsymbol{F}$ is affine, the basis functions can be written in terms of the global coordinates (x, y) in a simple fashion. With

$$\vartheta = ((x_2 - x_4)(y_1 - y_3) - (x_1 - x_3)(y_2 - y_4))^2 = (2|T|)^2,$$

where $|T|$ is the area of the physical element, and

$$x_{ik} = x_i - x_k,\ y_{ik} = y_i - y_k,\ d_{ij} = x_i y_j - x_j y_i,$$

we can formulate the basis functions for $\boldsymbol{W}_b^h$ in $\boldsymbol{x}$ on T as

$$\phi^1 = \frac{(2y_{13}x + 2x_{31}y + d_{13} + d_{43} + d_{14})(2y_{42}x + 2x_{24}y + d_{32} + d_{43} + d_{42})}{\vartheta},$$

$$\phi^2 = \frac{(2y_{42}x + 2x_{24}y + d_{12} + d_{41} + d_{42})(2y_{31}x + 2x_{13}y + d_{31} + d_{41} + d_{34})}{\vartheta},$$

$$\phi^3 = \frac{(2y_{13}x + 2x_{31}y + d_{12} + d_{13} + d_{23})(2y_{42}x + 2x_{24}y + d_{12} + d_{41} + d_{42})}{\vartheta},$$

$$\phi^4 = \frac{(2y_{31}x + 2x_{13}y + d_{21} + d_{31} + d_{32})(2y_{42}x + 2x_{24}y + d_{32} + d_{42} + d_{43})}{\vartheta}.$$

The fact that the approximation can be written as a polynomial in the global variable $\boldsymbol{x}$ will be of importance for the implementation.

Computing instead the basis functions $\{\varphi^j\}$ corresponding to the approximating space $\boldsymbol{W}_a^h$, we obtain, letting $d^i = 2|\Gamma^i|\vartheta$ and

$$\begin{aligned}\alpha &= x_3y_{12} + x_1y_{23} + x_2y_{31},\\ \beta &= x_4y_{32} + x_3y_{24} + x_2y_{43},\\ \gamma &= x_4y_{13} + x_1y_{34} + x_3y_{41},\\ \delta &= x_4y_{21} + x_2y_{41} + x_1y_{42},\end{aligned}$$

the basis as

$$\varphi^j = \boldsymbol{a}^j \cdot \boldsymbol{\phi},$$

where

$$\begin{aligned}\boldsymbol{\phi} &= (\phi^1, \phi^2, \phi^3, \phi^4),\\ \boldsymbol{a}^1 &= (2\vartheta - \alpha(\delta + 2x_2y_{14}), \alpha\beta, -\beta\gamma, \gamma\delta)/d^1,\\ \boldsymbol{a}^2 &= (\alpha\delta, 2\,\vartheta - \alpha\beta, \beta\gamma, -\gamma\delta)/d^2,\\ \boldsymbol{a}^3 &= (-\alpha\delta, \alpha\beta, 2\,\vartheta - \gamma\beta, \gamma\delta)/d^3,\\ \boldsymbol{a}^4 &= (\alpha\delta, -\alpha\beta, \beta\gamma, 2\,\vartheta - \gamma(\delta + 2x_2y_{14}))/d^4.\end{aligned}$$

5 Formulation of a discontinuous Galerkin method

Consider a subdivision of Ω into a geometrically conforming finite element mesh $\mathcal{T}_h = \{T\}$ of Ω, with h_T the diameter of triangle T and global mesh size parameter $h = \max_{T\in\mathcal{T}} h_T$. The set of edges in the mesh is denoted by $\mathcal{E} = \{E\}$ and we split $\mathcal{E}$ into three disjoint subsets

$$\mathcal{E} = \mathcal{E}_I \cup \mathcal{E}_D \cup \mathcal{E}_N,$$

where $\mathcal{E}_I$ is the set of edges in the interior of Ω, $\mathcal{E}_D$ is the set of edges on the Dirichlet part of the boundary $\partial\Omega_D$, and $\mathcal{E}_N$ is the set of edges in the Neumann part of the boundary $\partial\Omega_N$. Further, with each edge we associate a fixed unit normal $\boldsymbol{n}$ such that for edges on the boundary $\boldsymbol{n}$ is the exterior unit normal. We denote the jump of a function $\boldsymbol{v} \in \boldsymbol{W}_{a/b}^h$ at an edge E by $[\boldsymbol{v}] = \boldsymbol{v}^+ - \boldsymbol{v}^-$ for $E \in \mathcal{E}_I$ and $[\boldsymbol{v}] = \boldsymbol{v}^+$ for $E \in \mathcal{E}_D$, and the average $\langle\boldsymbol{v}\rangle = (\boldsymbol{v}^+ + \boldsymbol{v}^-)/2$ for $E \in \mathcal{E}_I$ and $\langle\boldsymbol{v}\rangle = \boldsymbol{v}^+$ for $E \in \mathcal{E}_D$, where $\boldsymbol{v}^\pm = \lim_{\epsilon\downarrow 0} \boldsymbol{v}(\boldsymbol{x} \mp \epsilon\,\boldsymbol{n})$ with $\boldsymbol{x} \in E$.

The discontinuous Galerkin method reads: find $(\boldsymbol{U}, P) \in \boldsymbol{W}_{a/b}^h \times L^h$ such that

$$a(\boldsymbol{U}, \boldsymbol{v}) + b(\boldsymbol{U}, q) + b(\boldsymbol{v}, P) + c(P, q) = l(\boldsymbol{v}, q) \quad \text{for all } (\boldsymbol{v}, q) \in \boldsymbol{W}_{a/b}^h \times L^h, \tag{3}$$

where the bilinear forms are defined by

$$\begin{aligned} a(\boldsymbol{U},\boldsymbol{v}) &= \sum_{T\in\mathcal{T}}(2\mu\,\boldsymbol{\varepsilon}(\boldsymbol{U}),\boldsymbol{\varepsilon}(\boldsymbol{v}))_T \\ &\quad -\sum_{E\in\mathcal{E}_I\cup\mathcal{E}_D}\left(\langle 2\mu\,\boldsymbol{\varepsilon}(\boldsymbol{U})\cdot\boldsymbol{n}\rangle,[\boldsymbol{v}]\right)_E+\left(\langle 2\mu\,\boldsymbol{\varepsilon}(\boldsymbol{v})\cdot\boldsymbol{n}\rangle,[\boldsymbol{U}]\right)_E \\ &\quad +2\mu\,\gamma\sum_{E\in\mathcal{E}_I\cup\mathcal{E}_D}(h^{-1}[\boldsymbol{U}],[\boldsymbol{v}])_E, \end{aligned} \tag{4}$$

$$b(\boldsymbol{v},q) = -\sum_{T\in\mathcal{T}}(q,\nabla\cdot\boldsymbol{v})_T+\sum_{E\in\mathcal{E}_I\cup\mathcal{E}_D}(\langle q\rangle,[\boldsymbol{v}\cdot\boldsymbol{n}_T])_E, \tag{5}$$

$$c(P,q)=\sum_{T\in\mathcal{T}}\left(\lambda^{-1}P,q\right)_T, \tag{6}$$

and the linear functional is defined by

$$l(\boldsymbol{v},q)=\sum_{T\in\mathcal{T}}(\boldsymbol{f},\boldsymbol{v})_T+\sum_{E\in\mathcal{E}_N}(\boldsymbol{h},\boldsymbol{v})_E. \tag{7}$$

Here $(\boldsymbol{v},\boldsymbol{w})_T=\int_T\sum_{ij}\boldsymbol{v}_{ij}\boldsymbol{w}_{ij}$, for 2-tensors $\boldsymbol{v},\boldsymbol{w}$; $(\boldsymbol{v},\boldsymbol{w})_E=\int_E\sum_i\boldsymbol{v}_i\boldsymbol{w}_i$, for vectors $\boldsymbol{v},\boldsymbol{w}$; h is defined by

$$h|_E=\left(|T^+|+|T^-|\right)/(2\,|E|)\quad\text{for } E=\partial T^+\cap\partial T^-, \tag{8}$$

with $|T|$ the area of T, on each edge. Note that the incompressible limit $\lambda\to\infty$ corresponds to $c(\cdot,\cdot)=0$.

Using Green's formula, we readily establish the following proposition.

Proposition 5.1 *The method* (3) *is consistent in the sense that*

$$a(\boldsymbol{u}-\boldsymbol{U},\boldsymbol{v})+b(\boldsymbol{u}-\boldsymbol{U},q)+b(\boldsymbol{v},P-p)+c(P-p,q)=0\quad\textit{for all } (\boldsymbol{v},q)\in\boldsymbol{W}^h_{a/b}\times L^h,$$

and $(\boldsymbol{u},p)$ *sufficiently regular.*

5.1 A priori error estimates

For the purpose of error analysis, we introduce the following mesh dependent energy norm

$$|||\boldsymbol{v}|||^2=\sum_{T\in\mathcal{T}}(2\mu\,\boldsymbol{\varepsilon}(\boldsymbol{v}),\boldsymbol{\varepsilon}(\boldsymbol{v}))_T+\sum_{E\in\mathcal{E}_I\cup\mathcal{E}_D}(h^{-1}[\boldsymbol{v}],[\boldsymbol{v}])_E. \tag{9}$$

We also introduce the edge norms

$$\|\boldsymbol{v}\|_E:=\|\boldsymbol{v}\|_{L^2(E)},\quad \|\boldsymbol{v}\|^2_{\mathcal{E}}:=\sum_{E\in\mathcal{E}_I\cup\mathcal{E}_D}\|\boldsymbol{v}\|^2_{L^2(E)}, \tag{10}$$

and the norm on L^h,

$$\|q\|_{L^h}^2 = \sum_{T\in\mathcal{T}_h} \|q\|_{L^2(T)}^2. \tag{11}$$

The mesh dependent norm $|||\cdot|||$ can be used to bound the broken $H^1(\Omega)$ norm on $\boldsymbol{W}_{a/b}^h$, which we show in the following proposition.

Proposition 5.2 *There is a constant c, independent of h, μ, and λ such that*

$$\sum_{T\in\mathcal{T}_h} \|\boldsymbol{v}\|_{H^1(T)}^2 \leq c|||\boldsymbol{v}|||^2 \quad \textit{for all } \boldsymbol{v}\in \boldsymbol{W}_{a/b}^h. \tag{12}$$

Proof. Assume that the right-hand side of (12) is zero. Note that $\|\boldsymbol{\varepsilon}(\boldsymbol{v})\|_{L^2(T)} = 0$, and thus $\boldsymbol{v}|_T \in \boldsymbol{RM}(T)$, where

$$\boldsymbol{RM}(T) = \{\boldsymbol{v}\in P^1(T):\ \boldsymbol{v}(\boldsymbol{x}) = \boldsymbol{a}_T + b_T\,(-x_2, x_1),\ \boldsymbol{a}_T\in\mathbb{R}^2,\ b_T\in\mathbb{R}\}, \tag{13}$$

is the space of linearized rigid body motions on T. Next, using $\|[\boldsymbol{v}]\|_{L^2(E)} = 0$, for all $E\in\mathcal{E}_I$, we conclude that there are constants $\boldsymbol{a}$ and b such that $\boldsymbol{a} = \boldsymbol{a}_T$ and $b = b_T$, for all triangles T. Furthermore, from $\|\boldsymbol{v}\|_{L^2(E)} = 0$ for $E\in\mathcal{E}_D$, it follows that $\boldsymbol{a} = \boldsymbol{0}$ and $b = 0$. Thus, if the right-hand side of (12) is zero, so is the left-hand side. Finally, finite dimensionality, together with scaling yields the result. □

As is well known, see Brezzi and Fortin [1], the existence of a solution to (3) satisfying optimal error estimates (also in the limit $\lambda\to\infty$) requires the following stability conditions:

1. There is a constant $\alpha \geq \alpha_0 > 0$ such that

$$\alpha|||\boldsymbol{v}||| \leq a(\boldsymbol{v},\boldsymbol{v}) \quad \text{for all } \boldsymbol{v}\in\boldsymbol{W}_{a/b}^h. \tag{14}$$

2. There is a constant $\beta\geq\beta_0 > 0$ such that

$$\beta \leq \inf_{q\in L^h}\ \sup_{\boldsymbol{v}\in\boldsymbol{W}_{a/b}^h} \frac{b(\boldsymbol{v},q)}{|||\boldsymbol{v}|||\ \|q\|_{L^h}}. \tag{15}$$

We shall first show that $a(\cdot,\cdot)$ is coercive with respect to the norm $|||\cdot|||$, given that γ is sufficiently large.

Proposition 5.3 *If $\gamma > c_0$, with c_0 sufficiently large, then the following estimates hold*

$$\alpha\,|||\boldsymbol{v}|||^2 \leq a(\boldsymbol{v},\boldsymbol{v}), \tag{16}$$

for all $\boldsymbol{v}\in\boldsymbol{W}_{a/b}^h$, where α is independent of h.

Proof. We first note that the following inverse estimate holds

$$\|h^{1/2}\langle \boldsymbol{n}\cdot\boldsymbol{\varepsilon}(\boldsymbol{v})\rangle\|_{\mathcal{E}}^2 \leq c\sum_{T\in\mathcal{T}}\|\boldsymbol{\varepsilon}(\boldsymbol{v})\|_T^2. \tag{17}$$

This inequality is proved by scaling and finite dimensionality. Furthermore, we have, for each $E\in\mathcal{E}_I\cup\mathcal{E}_D$, that

$$2(\langle \boldsymbol{n}\cdot\boldsymbol{\varepsilon}(\boldsymbol{v})\rangle\,,[\boldsymbol{v}])_E \leq 2\mu\delta\|h^{1/2}\,\langle \boldsymbol{n}\cdot\boldsymbol{\sigma}(\boldsymbol{v})\rangle\,\|_E^2+(2\mu\delta)^{-1}\|h^{-1/2}[\boldsymbol{v}]\|_E^2, \tag{18}$$

where we used the Cauchy-Schwarz inequality followed by the arithmetic-geometric mean inequality. Using this estimate we obtain

$$a(\boldsymbol{v},\boldsymbol{v})\geq(1-c\delta)\sum_{T\in\mathcal{T}}(2\mu\,\boldsymbol{\varepsilon}(\boldsymbol{v}),\boldsymbol{\varepsilon}(\boldsymbol{v}))_T+2\mu(\gamma-\delta^{-1})\|h^{-1/2}[\boldsymbol{v}]\|_{\mathcal{E}}^2.$$

Choosing δ small enough we obtain the Proposition follows. □

Remark 5.4 *It is also possible to drop the consistency terms involving the normal derivatives on the boundaries of the elements, following Rannacher and Turek [7]. For the analysis, we must then use Strang's second lemma which is not necessary in the present case. Note, however, that we cannot drop the jump term since it is crucial for stability (Proposition 5.2). This is an important difference from the Stokes problem, cf. [3].*

For brevity, we consider the inf-sup condition only for the approximating space $\boldsymbol{W}_a^h$. The case $\boldsymbol{U}\in\boldsymbol{W}_b^h$ will be treated in [4].

Proposition 5.5 *There is a constant $\beta>0$ such that*

$$\beta\leq\inf_{q\in L^h}\sup_{\boldsymbol{v}\in\boldsymbol{W}_a^h}\frac{b(\boldsymbol{v},q)}{|||\boldsymbol{v}|||\,\|q\|_{L^h}}. \tag{19}$$

Proof. For trial functions $(\boldsymbol{v},q)\in\boldsymbol{W}_a^h\times L^h$ we find that $(\langle q\rangle\,,[\boldsymbol{v}\cdot\boldsymbol{n}_T])_E=0$ for all E. In this case, the proof of (19) follows the lines of Rannacher and Turek [7]. □

We are now ready to state a standard a priori error estimate for the mixed method.

Theorem 5.6 *Let $(\boldsymbol{U},P)$ be the solution of (3) and $(\boldsymbol{u},p)$ the solution of (2) and let the assumptions in Propositions 5.3 and 5.5 hold. Then we have the error estimate*

$$|||\boldsymbol{U}-\boldsymbol{u}|||+\|P-p\|_{L^h}\leq Ch\Big(\|\boldsymbol{u}\|_{H^2(\Omega)}+\|p\|_{L_2(\Omega)}\Big).$$

Here the constant C depends on the constants α and β defined in Propositions 5.3 and 5.5, but is independent of h and μ.

Proof. The proof employs Proposition 5.1 and the approximation properties of the element, cf. Rannacher and Turek[7], with an additional trace inequality to handle the jump terms, cf. Hansbo and Larson[3]. We omit the details. □

6 Numerical examples

All examples in this section have been computed without the traction consistency terms; the approximation is thus close to the original RT, but with added jump terms. Further, we have employed the approximating space $\boldsymbol{W}_b^h$ (which is of no consequence on the affinely mapped elements used in the examples).

6.1 Stabilization

We first show that the RT element without stabilization can indeed be unstable. The problem is plane strain with Young's modulus $E = 10^3$ and Poisson's ratio $\nu = 0.3$ on the domain $(0,1) \times (0,3)$, with $\boldsymbol{u} = 0$ at $y = 0$, and a body load $\boldsymbol{f} = (1,0)$. Using only 3 elements for the discretization, we obtain an unstable solution (scaled numerical noise), Figure 3 (left), and adding the jump term (with $\gamma = 1$), the solution is stable, Figure 3 (right).

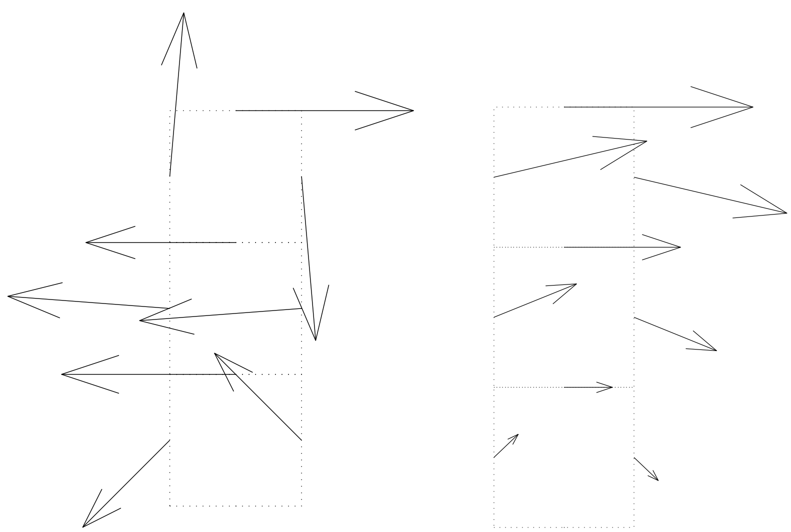

Figure 3: Solution without (left) and with jump term (right).

However, our experience is that the RT element is much less sensitive than the Crouzeix-Raviart element in this respect. This is expected, since there are more coupling terms between the nodes in the discrete operator for the RT element than there are for the CR element (notable if we, for instance, consider the case of a splitting of each quadrilateral into two triangles). In Figure 4 the mesh has been refined once, and the solution is stable without the jump terms.

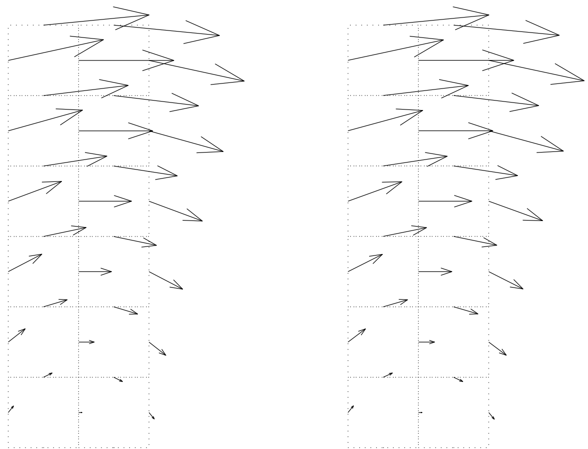

Figure 4: Solution without (left) and with jump term (right).

The effect of increasing γ is to make the problem stiffer, cf. Figure 5, where the mesh in Figure 4 is used. We show the effect of increasing γ on the maximum displacement. Clearly, γ should not be chosen too large (although the solution will still converge to the exact as the mesh is refined).

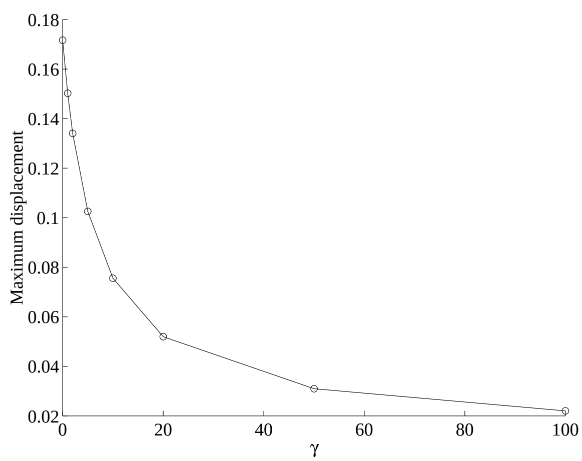

Figure 5: The effect of γ upon the maximum displacement.

6.2 The incompressible limit

We next consider the "driven cavity flow" problem, common in fluid flow applications. The domain is $\Omega = (0,1) \times (0,1)$, and the boundary conditions are given by: On $\partial\Omega_1 = \{x_2 = 1 \text{ and } 0 < x_1 < 1\}$ we set $\boldsymbol{u} = (1,0)$ and on $\partial\Omega \setminus \partial\Omega_1$ we set $\boldsymbol{u} = (0,0)$. In Figure 6 we show computational results for Young's modulus $E = 1$ and Poisson's ratio

$$\nu = \{0.4, 0.45, 0.5\}.$$

The method is completely robust with respect to locking.

References

[1] F. Brezzi and M. Fortin, *Mixed and Hybrid Finite Element Methods*, Springer Series in Computational Mathematics, 15, Springer Verlag, Berlin, 1991

[2] K. Arunakirinathar and B.D. Reddy, Some geometrical results and estimates for quadrilateral finite elements, *Comput. Methods Appl. Mech Eng.,* **122**, 307–314 (1995).

[3] P. Hansbo and M.G. Larson, Discontinuous Galerkin and the Crouzeix-Raviart element: Application to elasticity, Preprint 2000-09, The Finite Element Center, Chalmers University of Technology, Sweden.

[4] P. Hansbo and M.G. Larson, Discontinuous Galerkin and nonconforming quadrilateral elements, *to appear.*

[5] T.J.R. Hughes, *The Finite Element Method: Linear Static and Dynamic Finite Element Analysis*, Prentice-Hall, New Jersey, 1987

[6] J. Nitsche, Über ein Variationsprinzip zur Lösung von Dirichlet-Problemen bei Verwendung von Teilräumen, die keinen Randbedingungen unterworfen sind, *Abh. Math. Univ. Hamburg,* **36**, 9–15 (1970).

[7] R. Rannacher and S. Turek, A simple nonconforming quadrilateral Stokes element, *Numer. Methods Partial Differential Equations,* **8**, 97–111 (1992).

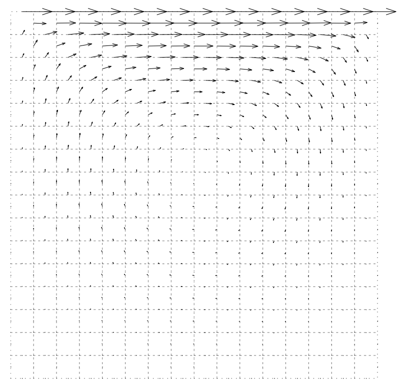

(a) $\nu = 0.3$

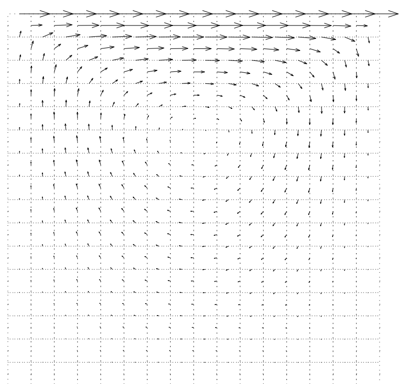

(b) $\nu = 0.45$

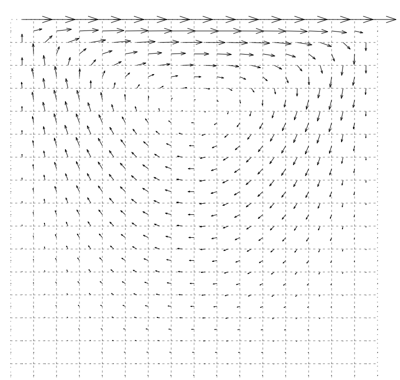

(c) $\nu = 0.5$

Figure 6: Poisson's ratio $\nu = 0.4$, 0.45, and 0.5.

Chalmers Finite Element Center Preprints

2000–01 *Adaptive Finite Element Methods for the Unsteady Maxwell's Equations*
Johan Hoffman

2000–02 *A Multi-Adaptive ODE-Solver*
Anders Logg

2000–03 *Multi-Adaptive Error Control for ODEs*
Anders Logg

2000–04 *Dynamic Computational Subgrid Modeling* (Licentiate Thesis)
Johan Hoffman

2000–05 *Least-Squares Finite Element Methods for Electromagnetic Applications* (Licentiate Thesis)
Rickard Bergström

2000–06 *Discontinuous Galerkin methods for incompressible and nearly incompressible elasticity by Nitsche's method*
Peter Hansbo and Mats G. Larson

2000–07 *A Discountinuous Galerkin Method for the Plate Equation*
Peter Hansbo and Mats G. Larson

2000–08 *Conservation Properties for the Continuous and Discontinuous Galerkin Methods*
Mats G. Larson and A. Jonas Niklasson

2000–09 *Discontinuous Galerkin and the Crouzeix-Raviart Element: Application to Elasticity*
Peter Hansbo and Mats G. Larson

2001–01 *A Simple Nonconforming Bilinear Element for the Elasticity Problem*
Peter Hansbo and Mats G. Larson

These preprints can be obtained from

`www.phi.chalmers.se/preprints`